JOURNAL OF CATALYSIS 103, 311–319 (1987)

The Oxidative Conversion of Methane to Higher Hydrocarbons over Alkali-Promoted Mn/SiO_2

C. ANDREW JONES, JOHN J. LEONARD, AND JOHN A. SOFRANKO[1]

ARCO Chemical Company, A Division of Atlantic Richfield Company, 3801 West Chester Pike, Newtown Square, Pennsylvania 19073

Received April 8, 1986; revised August 25, 1986

Increased yields of higher hydrocarbons from methane over manganese oxide–silica are obtained upon the addition of alkali metals and alkaline earths to the catalyst. Running redox cycles of alternating methane and air, a 15% manganese–5% sodium pyrophosphate–silica catalyst repeatedly gives a 17% yield of ethane, ethylene, and higher hydrocarbons (77% selectivity and 22% conversion) for 2 min at 850°C and 860 GHSV. This represents an improvement of 40 absolute percent selectivity over the alkali-free catalyst. The improvement arises largely by suppression of product oxidation. Further evidence is described for a mechanism involving surface-initiated gas phase methyl radicals.

INTRODUCTION

While progress has been made toward an efficient one-step process for oxidative conversion of methane to higher hydrocarbons, further improvements in catalyst performance are needed before commercial practice can be seriously considered. As the most unreactive hydrocarbon, methane demands novel treatment. The concept of a cyclic redox process has been described previously (*1–4*). Briefly, methane is oxidized to ethane and water by a metal oxide and the ethane reacts pyrolytically to ethylene and higher hydrocarbons in the first half of the cycle, then the metal oxide, so reduced, is reoxidized by air in the second half of the cycle. This fixed-bed cyclic process is similar to the Houdry process for dehydrogenation. Alternatively, the process may be carried out with a circulating, and continuously regenerated, moving or fluid bed (*5*). Work in other laboratories (*6–8*) has shown progress with a continuous, methane–air cofeed. Unlike the catalysts reported in the preceding paper (*3*), the improved catalysts reported here give product yields from continuous methane–air cofeed, competitive with those from cyclic redox operation (9). The cofeed results will be covered in a subsequent publication.

Manganese oxide on silica emerged as the best among the materials examined in the preceding paper (*3*) in terms of stability and productivity. By adding alkali metals or alkaline earths to that reagent, it has now been found that selectivity to carbon oxides can be reduced in favor of hydrocarbon products. In the case of sodium, carbon oxide selectivities are reduced by a factor of about 3 at the same methane conversion.

EXPERIMENTAL

Supported catalysts were prepared by incipient wetness impregnation of supports with aqueous solutions of manganese(II) acetate, alkali metal and alkaline earth acetates and nitrates, sodium pyrophosphate, and lanthanum nitrate.

Supports used were Houdry HSC 534 silica (250 m^2/g surface area), Norton SA 5551 α-alumina (0.4 m^2/g), United Catalysts T1746 γ-alumina (300 m^2/g), and a 50/50 silica–alumina prepared by coprecipitation (110 m^2/g).

[1] To whom correspondence and reprint requests should be addressed.

0021-9517/87 $3.00

Precipitated catalysts containing 1% or less sodium were prepared by base coprecipitation of a methanolic solution of tetraethoxysilane and manganese and sodium acetates. Precipitated catalysts containing higher levels of sodium were prepared by rapid mixing of and precipitation from solutions of manganese acetate and sodium silicate, followed by water washing to reach the desired level of sodium. All catalysts were calcined in air at 850°C except where noted.

Quartz tube reactors were used and product analysis was primarily by gas chromotography, as described previously (*3*). Instantaneous results were obtained with syringe sampling, and cumulative results were obtained with gas bags. For the lead mirror experiments, the mirrors were deposited on inside walls of quartz tubes by pyrolyzing tetrabutyl lead vapor carried in a nitrogen stream.

TABLE 1

Addition of Third Components to 10% Manganese on Silica

Wt%	Surface area[a] (m^2/g)	% Conversion[b]	% Selectivity[b]
0.05 Na[c]	98	7	57
0.22 Na	61	8	53
1.7 Na	0.6	13	86
4.2 Na	0.4	4	92
0.5 Li	8	7	76
2.9 K	50	7	72
6.3 Rb	56	10	71
9.7 Cs	71	8	69
1.8 Mg	68	6	72
3.0 Ca	56	4	70
10.0 Ba	47	12	62
3.4 La	60	9	63
10.3 La	38	9	41

[a] After 10–20 methane runs
[b] The fifth 2-min methane run at 800°C, 860 GHSV.
[c] Contained in blank silica as received.

RESULTS

After extensive screening of metal oxide catalysts (*3*), manganese oxide was chosen for further development because of its reactivity and lack of volatility at operating conditions. In that work, better selectivity to higher (C_{2+}) hydrocarbons was observed with silica as the support than with alumina. One reason for this may be the higher acidity of alumina which promotes destructive interaction of olefins with the catalyst surface. This hypothesis led to the screening of alkali metals and alkaline earths as additives to the 10% manganese–silica system. Results are listed in Table 1 for Li, Na, K, Rb, Cs, Mg, Ca, and Ba, all at the same molar concentration as 1.7% sodium. The table also includes three other sodium levels, and two levels of lanthanum corresponding to the same molar concentration and the same concentration of cationic charge as 1.7% sodium. The highest C_{2+} yield was obtained with 1.7% sodium as promoter. In some cases, results changed markedly between the first two runs, but by the fifth run, performance was stable enough to draw meaningful conclusions.

It was found that inclusion of phosphorus as sodium pyrosphosphate (5%) led to greater stability than catalysts prepared from sodium acetate at the same sodium level (1.7%). Table 2 provides evidence that the effect of phosphorus may be related to enhanced retention of surface area. A series of catalysts was then prepared with 15% manganese and a range of sodium pyrosphosphate loadings. Their performance is plotted in Fig. 1 as a function of sodium content. The leftmost point in the figure and the first entry in Table 1 represent manganese–silica catalysts with no added sodium, but 0.05% sodium contained in the silica as received. As sodium content increases, first activity increases, then selectivity. Above about 0.5% sodium, activity slowly falls while selectivity slowly rises. The conversion–selectivity relationship changes little above 0.5% sodium and is plotted in Fig. 2 for the 1.7% sodium catalyst which was studied extensively. Com-

TABLE 2

Effects of Phosphorus on 10% Manganese, 1.7% Sodium on Silica

Loading on SiO_2	Run 1[a]			Run 25[a]		
	% Conversion	% Selectivity	Surface area (m^2/g)	% Conversion	% Selectivity	Surface area (m^2/g)
10% Mn, 1.7% Na	15	82	1.0	6	91	0.6
10% Mn, 1.7% Na (as 5% $Na_4P_2O_7$)	18	80	2.2	12	88	1.0

[a] Two minutes, 800°C, 860 GHSV.

parison with the unpromoted catalyst shows a marked difference in performance. Detailed selectivities are listed in Table 3 for runs on three representative catalysts. While selectivity to C_3 and higher hydrocarbons never exceeded that to C_2's, the ratio of C_{3+} to C_2's did increase upon the addition of sodium. Most of the C_3's was propylene, C_4's butadiene, and C_5's linear and branched dienes.

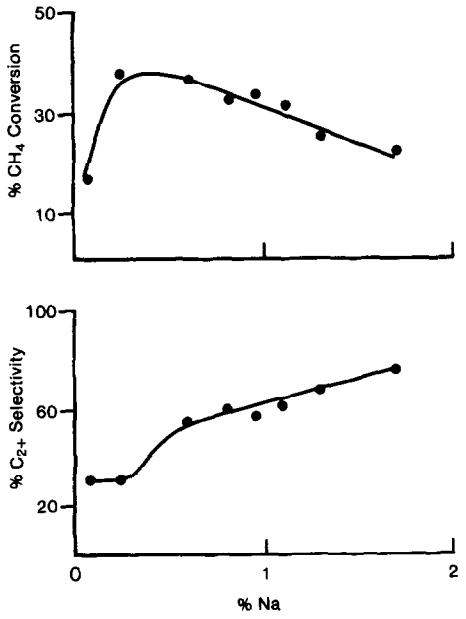

FIG. 1. Cumulative results of 2-min runs at 850°C and 860 CH_4 GHSV over 15% Mn/SiO_2 as a function of Na loading (applied as $Na_4P_2O_7$).

Cumulative results listed in Tables 1–5, derived from gas bag collection of entire methane cycles, represent time-average conversion and conversion-weighted selectivity. The instantaneous time dependence of a typical run with the 15% manganese, 5% sodium pyrophosphate on silica catalyst is plotted in Fig. 3. Instantaneous results for six different catalysts are plotted in Fig. 4. Catalysts which are selective throughout a run, at high initial conversion as well as later low conversion, produce better cumulative results. Notice that the better catalysts, e.g., the upper three in Fig. 4, display a more gradual falloff of conversion with time. The catalyst labeled Mn_2SiO_4 is a coprecipitate described below.

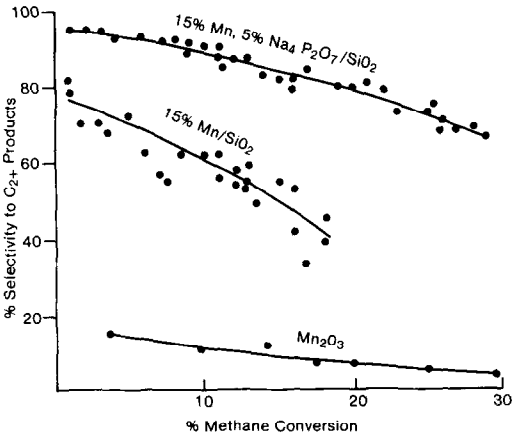

FIG. 2. Cumulative results of 2-min CH_4 runs at 800–850°C and 400–7000 GHSV.

TABLE 3

Typical Product Selectivities[a]

	10% Mn/SiO_2	10% Mn, 1.7% Na/SiO_2	15% Mn, 5% $Na_4P_2O_7/SiO_2$
Temperature (°C)	*800*	*800*	*850*
% CH_4 conversion	7	9	22
% Selectivity to			
C_2H_4	31	47	47
C_2H_6	20	30	14
C_3[b]	3	7	6
C_4[b]	1	4	4
C_5[b]	0.1	0.7	1
Benzene	0.4	0.9	4
Toluene	0.1	0.2	0.4
CO	13	5	11
CO_2	30	5	11
Coke	1	0.5	1

[a] Two-minute methane runs, 860 GHSV.
[b] Primarily olefinic.

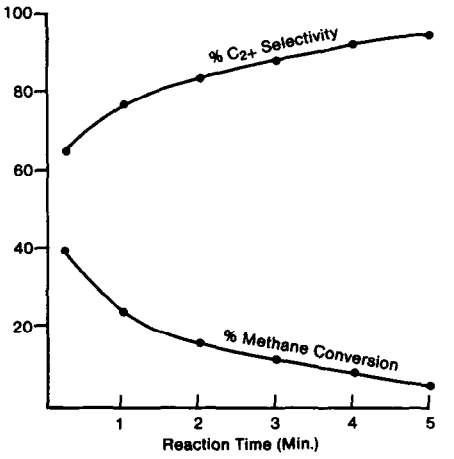

FIG. 3. Instantaneous results at 850°C and 860 CH_4 GHSV over 15% Mn, 5% $Na_4P_2O_7/SiO_2$.

Aluminas and a silica–alumina were substituted for silica as support. While addition of sodium improved the results for both silica and alumina, silica ultimately produced the highest yields of hydrocarbons (Table 4). Since it was observed that the more selective silica catalysts, i.e., those with added sodium, have surface areas less than 2 m^2/g, experiments were done to test the possibility that low surface area is the nec-

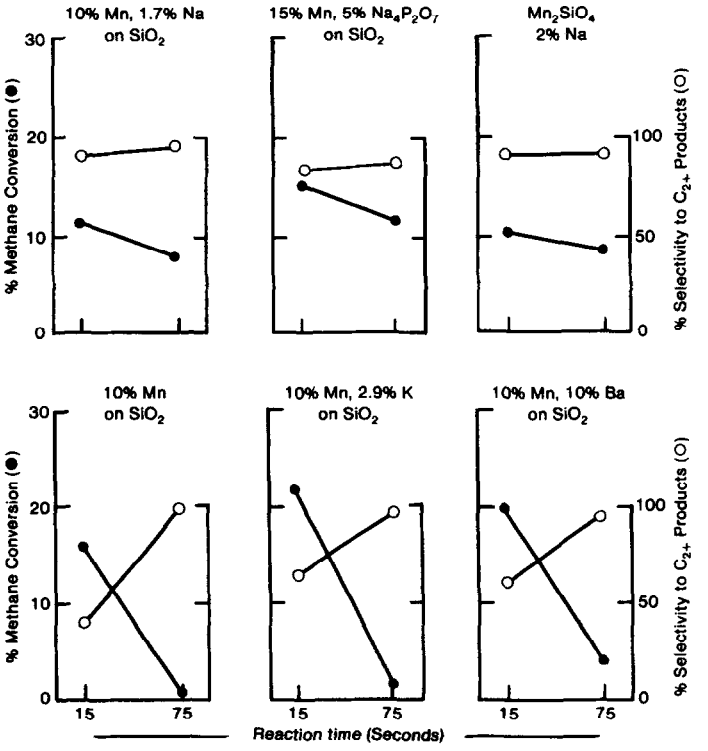

FIG. 4. Instantaneous results at 800°C and 860 CH_4 GHSV.

TABLE 4

Manganese and Sodium on Various Supports

Support	Wt% Mn	Wt% Na	Surface area[a] (m^2/g)	% Conversion[b]	% Selectivity[b]
SiO_2	10	0.05	98	7	57
SiO_2[c]	10	0.05	0.6	11	35
SiO_2[d]	10	0.05	4	3	80
SiO_2	10	1.7	0.6	13	86
α-Al_2O_3	10	0.06	0.4	13	49
α-Al_2O_3	10	1.7	0.2	12	74
γ-Al_2O_3	10	1.7	49	7	5
γ-Al_2O_3	10	4.2	27	11	6
SiO_2–Al_2O_3	10	1.7	1.5	9	25

[a] After 10–20 methane runs.
[b] The fifth 2-min methane run at 800°C, 860 GHSV.
[c] SiO_2 first calcined at 1000°C, then loaded with manganese.
[d] Catalyst calcined at 1000°C after manganese loading.

essary characteristic and not the presence of sodium, the sole function of which is the reduction of surface area. Two manganese–silica catalysts without added sodium were prepared with low surface area by calcination at 1000°C, one before manganese loading and the other after. The inferior results in Table 4 for these catalysts show that low surface area is not a sufficient condition for high selectivity. Sodium must play an additional role.

The dramatic effect of sodium on manganese oxide is demonstrated in Table 5. Bulk manganese oxide (0.5 m^2/g) was carried though a series of runs (Fig. 2) and found to be almost completely nonselective. Sodium permanganate was then similarly run and found to obey a conversion–selectivity relationship close to that of the better sodium–manganese–silica catalysts. After use, this material was found to contain β-$NaMnO_2$ and β-$Na_{0.7}MnO_2$ by X-ray diffraction. Manganese oxide was then loaded with sodium at sodium : manganese ratios between zero and one. In this series, selectivity increased monotonically at comparable conversions as the ratio increased.

Sodium manganese oxides were not observed in XRD patterns of sodium–manganese–silica catalysts; however, the latter catalysts did display strong XRD patterns for Mn_7SiO_{12} (braunite) and quartz when oxidized and a strong quartz and weak Mn SiO_3 pattern when reduced. In an attempt to identify the active, selective species, coprecipitates of manganese: silica ratios of 7:1, 2:1, and 1:1 were prepared, corresponding to known mineral manganese silicates and species observed by XRD. None of these combinations was selective until sodium was added (Table 5).

The atomic ratio of available, or active, oxygen to manganese was calculated from product yields of extended methane runs in which the sodium–manganese–silica catalyst was completely reduced. The ratio was also determined gravimetrically by cyclic hydrogen reduction and air oxidation of the catalysts at 800°C in a Cahn microbalance. Both methods produced a ratio of 0.4, the same value as previously determined for manganese–silica without added sodium (*3*). This is consistent with the value (0.43) for reduction of Mn_7SiO_{12} to $MnSiO_3$, the species observed by XRD.

$$Mn_7SiO_{12} + 6SiO_2 \rightleftarrows 7MnSiO_3 + 3O$$

Scanning electron microscopy revealed a clear difference in surface morphology between the manganese–silica systems with and without added sodium. The latter appeared very rough with sharp angles and discontinuities at particle boundaries, while

TABLE 5

Effect of Sodium and Silicon on Manganese Oxide

	Wt% Na	% CH_4 conversion[a]	% C_{2+} selectivity[a]
MnO_x	0	42	1
$NaMnO_x$	21	12	85
Mn_7SiO_x	0	35	10
Mn_2SiO_x	0	25	12
Mn_2SiO_x	2	15	82
$MnSiO_x$	0	31	10
$MnSiO_x$	1	14	49
$MnSiO_x$	2	7	94
$MnSiO_x$	9	2	93

[a] Fifth 2-min methane run at 800°C, 860 GHSV.

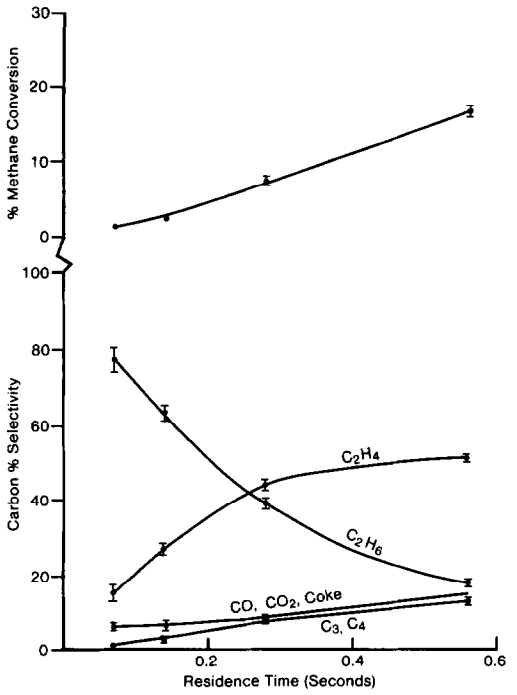

FIG. 5. One-minute cumulative data for CH_4 feed over 15% Mn, 5% $Na_4P_2O_7/SiO_2$ at 825°C.

the former appeared very smooth, as if particles had melted together into a continuous network.

A series of 1-minute methane runs was carried out over 15% manganese, 5% sodium pyrophosphate on silica to determine the effect of residence time on selectivity. The same series was repeated with a feed of 10 vol.% ethylene in methane. The results are plotted in Figs. 5 and 6, respectively. Extrapolation to zero residence time of selectivity trends in the methane runs identifies ethane as the major product (95%) with a small selectivity to carbon oxides (5%). A similar extrapolation of the methane–ethylene runs again includes ethane (30%) and carbon oxides (10%) as products, but in this case, butene (20%) persists and propylene (40%) appears to be the major product. Selectivities to C_5's, benzene, and toluene, not plotted for simplicity, fall to zero at short residence times. The majority of carbon oxides formed at longer residence times arises from secondary reactions. Coke selectivities, plotted with carbon oxides for simplicity, are consistently 10 or more times smaller than those of carbon oxides. The trends are similar to those observed previously (*3*) in the absence of added sodium. One difference is the considerably higher selectivity to carbon oxides and coke at long residence times without added sodium.

Paneth lead mirror experiments (*10*) were performed to test the mechanism put forth previously (*3*) that gas phase methyl radicals are the primary species formed from methane oxidation. Methane runs were made in the same reactor at 800°C and 1000 GHSV, first with silica as catalyst and then with 15% manganese, 5% sodium pyrophosphate on silica. The exit of the reactor tube, outside of the furnace, was tapered so that a high product gas velocity, 13 m/sec, was achieved (Fig. 7).

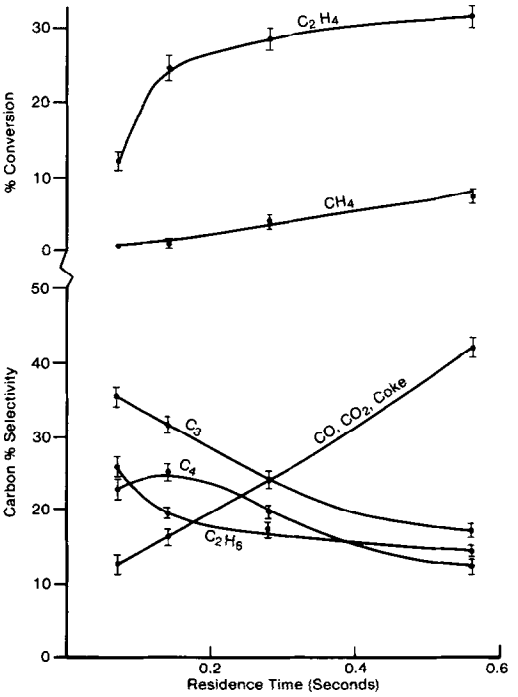

FIG. 6. One-minute cumulative data for a feed of 10 vol.% C_2H_4 in CH_4 over 15% Mn, 5% $Na_4P_2O_7/SiO_2$ at 825°C.

FIG. 7. Quartz reactor tube used for lead mirror experiments. The large diameter and tapered sections were inside the furnace, the small diameter section was outside.

First, a lead mirror was deposited in the exit zone. Then 16 consecutive methane–nitrogen–air–nitrogen cycles were carried out over silica. The hottest part of the lead mirror, 3 mm long, disappeared by lead sublimation. With this as a baseline, 16 runs were carried out over the sodium–manganese–silica catalyst with a new lead mirror in place. This time, 15 mm of the lead mirror disappeared, a distance well into the cooler length of the tube, below 200°C. The mechanistic implications are discussed below.

DISCUSSION

The improvement in selectivity upon addition of sodium to the manganese–silica system could arise for a number of reasons. There is evidence for beneficial effects of surface basicity, a specific sodium–manganese interaction, and reduction of surface area. These solid phase aspects will be treated in turn, followed by a discussion of the gas phase chemistry.

In general, improved performance can be correlated with catalyst basicity. While sodium caused the greatest improvement, all the alkali metals and alkaline earths in Table 1, when added to the manganese–silica system, improved activity or selectivity, or both. Except for sodium and lithium, this improvement came with only a modest decrease in surface area, and in no case were there any species evident from XRD, other than quartz, cristobalite, Mn_7SiO_{12}, or $MnSiO_3$. With no added alkali or alkaline earth, surface area reduction by high temperature calcination did not improve product yields to levels obtained with the base-promoted catalysts, regardless of surface area (Tables 1 and 4). Inferior yields with alumina and silica–alumina supports also reflect the need for low acidity. It can be reasonably argued that acidic surfaces would tend to interact more than neutral or basic ones with olefinic and aromatic products. Once activated at these high temperatures, such products are prone to coking or overoxidation by the oxidizing surface.

Bulk manganese oxide, not acidic and of low surface area (0.5 m^2/g), proved to be the most nonselective material examined. With the addition of sodium, selectivity improved dramatically and sodium manganese oxides appeared in XRD. While these species did not appear in XRD of the sodium–manganese–silica, it may be that, in this case, amorphous species of this type were formed, since no crystalline, sodium-containing species at all were observed. In addition, Mn_3O_4 was observed by XRD in manganese–silica without added sodium, and it disappeared upon sodium addition. These differences point toward a sodium–manganese interaction which affects the tendency of manganese oxide to overoxidize reactive hydrocarbons.

In addition to basicity and sodium–manganese interaction, surface area influences catalyst performance. The lowest surface area and highest yield in Table 1 results from sodium promotion. Even within the aluminas, low surface area α-alumina works much better than high surface area γ-alumina. The variation in reaction rates in Fig. 4 is probably a consequence of surface area. The three catalysts represented in the bottom half of the figure have much higher surface areas than the upper three and as a result, they have higher initial activity. Having spent more active oxygen in the early part of the run, the activity of these catalysts falls off more rapidly. While the cumulative conversion might be the same for a 2-minute run on a low surface area and a high surface area catalyst, the bulk of conversion in the high surface area case takes place quicker at higher instantaneous

conversion and correspondingly lower selectivity. This effect is in addition to the fact that, even at the same instantaneous conversion, selectivity is better with sodium promotion. The latter effect is, in part, a result of the fact that higher surface areas give proportionately higher rates of product coking and subsequent combustion.

The gas phase chemistry should be independent of catalyst promotion. The improvement in selectivity realized by sodium promotion, an overall increase in hydrocarbons at the expense of carbon oxides and coke, leaves the distribution of hydrocarbons qualitatively unchanged from that produced by the unpromoted catalyst (Table 3). In addition, the results of the variation of residence time (Fig. 5) lead to the same general conclusions as reached earlier (*3*) for the unpromoted catalyst. As discussed in that case, the interpretation of short residence time selectivities as representing the primary product distribution may be too simplistic, since heavier products can form and crack back to light products on the way to thermodynamic equilibrium, thus masking the primary distribution. In fact, selectivity to C_3–C_7 products drops from 16 to 1% as residence time drops through the range shown in Fig. 5. At short residence times, heavy intermediates thus become less important and selectivity trends reflect at least an approach to the primary distribution. Ethane is apparently the major primary product. The selectivity to carbon oxides, at short residence times, is three to four times greater without sodium promotion, implying a greater propensity for destruction of methyl radicals. At long residence times the selectivity to carbon oxides and coke is still three times greater for the unpromoted catalyst, implying a greater propensity for product destruction. The qualitative trends, however, are the same for the two catalysts. The gas phase mechanism advanced previously (*3*) is still satisfactory: methane is oxidized to methyl radicals, which dimerize in the gas phase to ethane, which dehydrogenates to ethylene which can then add a methyl radical or dimerize, and so on.

These ideas are supported by results with 10% ethylene-in-methane feed (Fig. 6). For both catalysts, propylene appears to be the major primary product, having formed presumably by addition of methyl radicals to ethylene. Ethylene conversion rises steeply with increasing residence time and then levels off as its production rate from methane and heavier product cracking approaches its conversion rate.

Methyl radicals have been detected in related work on methane in the presence of gas phase oxygen (*11*). In the absence of gas phase oxygen, gas phase methyl radicals would have to have been formed at a surface before passing into the gas phase. Surface-generated radicals have been observed from butane over manganese catalysts (*12*). In addition to the indirect kinetic evidence for methyl radicals described above, more evidence was obtained from cyclic methane runs, described earlier, in which the movement of a 15 mm length of a thin film of lead downstream from the catalyst was observed. This movement of lead could have been caused by a variety of radicals, but reasonable alternatives to methyl radicals, e.g., ethyl or propyl, dissociate to a hydrogen atom and the appropriate olefin too rapidly to be of concern (*13*). Methyl radicals would have a lifetime adequate to cause the observed movement of lead. A steady-state methyl radical concentration of 6×10^{-10} mole/ml would exist under the run conditions if produced at the observed methane conversion rate of 4×10^{-6} mole/ml sec^{-1} and removed with a recombination rate constant of 1×10^{13} ml/mol sec^{-1} (*14*). This concentration, upon leaving the catalyst bed, would have a half-life of 0.2 msec, a quarter-life of 0.5 msec, and a tenth-life of 1.5 msec, corresponding to distances of 2, 7, and 20 mm travel down the tube. Recall that the observed lead migration distance was 15 mm. Although this is a simplistic analysis, the weight of evidence strongly fa-

vors a mechanism involving surface-initiated gas phase methyl radicals as building blocks for higher hydrocarbons.

CONCLUSIONS

Methane conversion catalysts based on manganese and silica can be improved by a combination of increasing surface basicity and decreasing surface area. In particular, sodium is well suited for these two requirements, as well as conversion of nonselective manganese oxide into a more selective form. The pyrophosphate anion provides greater stability to the catalyst. A catalyst of 15% manganese and 5% sodium pyrophosphate on silica has been used to obtain a 17% yield (22% conversion, 77% selectivity) of higher hydrocarbons for 2 min at 850°C and 860 GHSV in repetitive cyclic methane runs alternating with air reoxidation of the catalyst.

The observed kinetics are consistent with a mechanism involving the oxidation of methane by a surface oxide to methyl radicals and water. Building of higher hydrocarbons then follows a thermal, gas phase radical sequence. Nonselective products are formed primarily by destruction of methyl radicals at low methane conversion and destruction of olefinic and aromatic products at high conversion.

REFERENCES

1. Mitchell, H. L., III, and Waghorne, R. H., U.S. Patents 4,172,810 (1979); 4,205,194 (1980); and 4,239,658 (1980) to Exxon Res. and Eng. Co.
2. Keller, G. E., and Bhasin, M. M., *J. Catal.* **73,** 9 (1982).
3. Sofranko, J. A., Leonard, J. J., and Jones, C. A., *J. Catal.* **103,** 302 (1987).
4. Jones, C. A., and Sofranko, J. A., U.S. Patent 4,499,322 (1985) to Atlantic Richfield Co.
5. Jones, C. A., Leonard, J. J., and Sofranko, J. A., U.S. Patent 4,560,821 (1985) to Atlantic Richfield Co.
6. Otsuka, K., Jinno, K., and Morikawa, A., *Chem. Lett.* 499 (1985).
7. Ito, T., Wang, J. X., Lin, C. H., and Lunsford, J. H., *J. Amer. Chem. Soc.* **107,** 5062 (1985).
8. Hinsen, W., and Baerns, M., *Chem. Zig.* **107,** 223 (1983).
9. Jones, C. A., Leonard, J. J., Sofranko, J. A., and Withers, H. P., U.S. Patent 4,523,049 (1985) to Atlantic Richfield Co.; Jones, C. A., and Sofranko, J. A., U.S. Patent 4,523,050 (1985) to Atlantic Richfield Co.
10. Paneth, F., and Hofeditz, W., *Ber. Dtsch. Chem. Ges. B* **62,** 1335 (1929).
11. Driscoll, D. J., and Lunsford, J. H., *J. Phys. Chem.* **89,** 4415 (1985).
12. Kolts, J. H., and Delzer, G. A., *Science* **232,** 744 (1986).
13. Sundaram, K. M., and Froment, G. F., *Ind. Eng. Chem. Fundam.* **17,** 174 (1978).
14. Clark, T. C., Izod, T. P. J., and Kistiakowsky, G. B., *J. Chem. Phys.* **54,** 1295 (1971).